

Phosphorus-31 Solid-State NMR of a Phosphine–Borane Adduct: Phosphorus Chemical Shielding Trends in the Isoelectronic Series R_3PX , where $X = BH_3, CH_2, NH, O$

William P. Power

Contribution from the Guelph–Waterloo Center for Graduate Work in Chemistry, Department of Chemistry, University of Waterloo, Waterloo, Ontario N2L 3G1, Canada

Received September 13, 1994[®]

Abstract: The orientation of the phosphorus chemical shift tensor and the magnitudes of its principal components in solid triphenylphosphine–borane adduct were determined from the ^{31}P chemical shift ^{11}B -dipolar-coupled NMR powder lineshape. Although the ^{31}P isotropic chemical shift of the adduct was similar to that of triphenylphosphine oxide, the anisotropic chemical shift parameters revealed substantial differences in the local electronic environment surrounding the phosphorus nucleus. The orientation-dependence of the ^{31}P – ^{11}B dipolar coupling indicated that the most shielded component of the phosphorus chemical shift tensor lies close to the P–B bond and provided a P–B bond length of $1.95 \pm 0.02 \text{ \AA}$, in good agreement with diffraction data. *Ab initio* calculations of the phosphorus chemical shielding tensors for the isoelectronic series of trimethylphosphine derivatives, $(CH_3)_3PX$, $X = BH_3, CH_2, NH, O$, provide considerable detail concerning the sensitivity of the three principal components to changes in the X group. Only the most shielded component, σ_{33} , which lies along the P–X bond, is dominated in an exclusive and consistent fashion by the X group, linearly with respect to the P–X bond length.

Introduction

Phosphorus chemical shifts in phosphine derivatives have undergone serious examination and attempted interpretation for over 30 years,^{1–3} yet their seemingly random variation has defied a unifying explanation. Proposed models have included arguments based on electronegativities of substituents, π -electron overlap, phosphine cone angles, *etc.* The relatively recent increase in solid-state NMR studies of phosphine derivatives⁴ has permitted experimentalists to determine the anisotropic ^{31}P chemical shift parameters, which has provided a clearer picture of magnetic shielding than is available from isotropic shifts alone determined with high-resolution NMR. Within the last several years, *ab initio* calculations of chemical shielding tensors have emerged as a reliable technique for predicting and analyzing the trends in chemical shielding tensors for many nuclei, particularly ^{13}C , ^{15}N , and ^{29}Si .^{5–7} The rapid increase in computational power has provided facilities capable of predicting chemical shielding reliably for nuclei such as ^{31}P as well. Here an attempt is made to develop a better understanding of the trends in phosphorus chemical shifts of several computationally accessible phosphine derivatives using the combination of experimental determination and theoretical prediction of the orientation and magnitudes of the principal components of the complete phosphorus chemical shielding tensor.

This study will focus on the factors controlling the phosphorus shifts in the isoelectronic series, R_3PX , where $X = BH_3, CH_2, NH$ and O . The P–X bond lengths become increasingly shorter

through this series, with average values of approximately 1.90, 1.70, 1.58, and 1.45 Å for the P–B, P–C, P–N, and P–O bonds, respectively. This trend has been interpreted as an increase in the P–X bond order due to larger “back-bonding” contributions from the X atoms. In contrast to the trend of decreasing bond lengths in the above P–X series, the ^{31}P chemical shifts for these compounds show no clear basis for differences in the P–X bond orders, as all shifts fall within the range typical for phosphines (+150 to –100 ppm⁸), *e.g.*, $\delta_{iso}((CH_3)_3^{31}PO) = 36.2 \text{ ppm}$,⁹ $\delta_{iso}((CH_3)_3^{31}PNH) = 12.8 \text{ ppm}$,¹⁰ $\delta_{iso}((CH_3)_3^{31}PCH_2) = -2.1 \text{ ppm}$,¹¹ and $\delta_{iso}((CH_3)_3^{31}PBH_3) = -1.8 \text{ ppm}$.¹² This differs from the trends observed for first row atoms such as carbon and nitrogen, where an increase in bond order from 1 to 2 is associated with a significant deshielding of the ^{13}C or ^{15}N isotropic chemical shift.¹³ For example, the ^{13}C isotropic chemical shift in ethane is 9 ppm,¹⁴ while that for ethylene is 126 ppm.¹⁵ An even better example is provided by nitrogen shifts,¹⁶ which vary from –400 ppm in ammonia¹⁷ to –265 ppm in the amide glycylglycine·HCl·H₂O¹⁸ to 152 ppm in azobenzene,¹⁹ where the bond order varies from 1 to 1.5 to 2. The deshielding also contributes to large differences in the anisotropies of the carbon and nitrogen chemical shift tensors, which increase from 7 ppm in ethane to 210 ppm in ethylene

(8) Dixon, K. R. In *Multinuclear NMR*; Mason, J., Ed.; Plenum: New York, 1987; p 369.

(9) Kblischek, A.; Hausen, H. D.; Weidlein, J.; Binder, H. Z. Z. *Naturforsch.* **1983**, *38B*, 1046.

(10) Schmidbaur, H.; Buchner, W.; Scheutzw, D. *Chem. Ber.* **1973**, *106*, 1251.

(11) Schmidbaur, H.; Scherm, H. P. Z. *Anorg. Allg. Chem.* **1979**, *459*, 170.

(12) Cowley, A. H.; Damasco, M. C. *J. Am. Chem. Soc.* **1971**, *93*, 6815.

(13) Duncan, T. M. *A Compilation of Chemical Shift Anisotropies*; Farragut: Madison, WI, 1990.

(14) Solum, M. S.; Facelli, J.; Michl, J.; Grant, D. M. *J. Am. Chem. Soc.* **1986**, *108*, 6464.

(15) Zilm, K. W.; Conlin, R. T.; Grant, D. M.; Michl, J. *J. Am. Chem. Soc.* **1980**, *102*, 6672.

(16) Mason, J. In *Multinuclear NMR*; Mason, J., Ed.; Plenum: New York, 1987; p 335.

(17) Kukolich, S. G. *J. Am. Chem. Soc.* **1975**, *97*, 5704.

(18) Harbison, G. S.; Jelinski, L. W.; Stark, R. E.; Torchia, D. A.; Herzfeld, J.; Griffin, R. G. *J. Magn. Reson.* **1984**, *60*, 79.

[®] Abstract published in *Advance ACS Abstracts*, January 15, 1995.

(1) Lechter, J. H.; Van Wazer, J. R. *J. Chem. Phys.* **1966**, *44*, 815.

(2) Pregosin, P. S.; Kunz, R. W. In *NMR Basic Principles Progress*; Diehl, P., Fluck, E., Kosfeld, R., Eds.; Springer-Verlag: Berlin, 1979; Vol. 16.

(3) Gorenstein, D. G. *Prog. Nucl. Magn. Reson. Spectrosc.* **1983**, *16*, 1.

(4) Davies, J. A.; Dutremez, S. *Coord. Chem. Rev.* **1992**, *114*, 61.

(5) Facelli, J.; Grant, D. M. In *Topics in Stereochemistry*; Eliel, E. L., Wilen, S. H., Eds.; J. Wiley: New York, 1989; Vol. 16, p 1.

(6) Kutzelnigg, W.; Fleischer, U.; Schindler, M. In *NMR Basic Principles and Progress*; Diehl, P., Fluck, E., Kosfeld, R., Eds.; Springer-Verlag Berlin, 1990; Vol. 23, p 165.

(7) See also, *Nuclear Magnetic Shieldings and Molecular Structure*; Tossell, J. A., Ed.; Kluwer Academic: Dordrecht, 1993.

and from 40 ppm in ammonia to 150 ppm in the amide to 925 ppm in azobenzene. If the trends in the P–X bond lengths are due to increases in the bond order, then some investigation of the ³¹P chemical shift tensors in these compounds is necessary to determine the behavior of the chemical shift anisotropies and to understand the apparent *insensitivity* of the ³¹P isotropic chemical shift to the changes in P–X bond order. In this study, the ³¹P chemical shift tensors have been investigated through the series of R₃P–X compounds using new and existing experimental data for the triphenylphosphines and the results of new *ab initio* calculations of the chemical shielding tensors in a related series of trimethylphosphine derivatives using the local origin local orbital (LORG) formalism.²⁰

Experimental Section

Triphenylphosphine–borane and triphenylphosphine were obtained from the Aldrich Chemical Company. Triphenylphosphine–borane was recrystallized from tetrahydrofuran prior to use, while triphenylphosphine was used without further purification.

All solid-state NMR spectra were obtained at 11.7 T and 295 K on a Bruker AMX-500 NMR spectrometer, operating at 500.13 MHz for ¹H, 202.46 MHz for ³¹P, and 160.62 MHz for ¹¹B. The ³¹P cross-polarization (CP) spectra with high-power ¹H decoupling utilized ¹H $\pi/2$ pulse widths of 2.5 μ s, followed by contact times of approximately 3 ms. Spectral widths of 50 to 100 kHz were used for the ³¹P spectra. Spin–lattice relaxation times were determined using the standard inversion-recovery pulse sequence without cross-polarization and with high-power proton decoupling during acquisition. The ³¹P $\pi/2$ pulse width was 2.8 μ s. The ³¹P spectra were referenced to 85% H₃PO₄(aq) using an external sample of solid NH₄H₂PO₄, which has a ³¹P isotropic chemical shift of +0.81 ppm. The ¹¹B spectra were referenced to an external solution sample of Et₂O·BF₃. Dwell times of 0.2 μ s, corresponding to 2.5 MHz spectral widths, were used to collect the ¹¹B MAS spectra, with ¹¹B pulses of 0.3–0.5 μ s ($< \pi/10$ pulse) to ensure equal excitation of the satellite and central transitions. All magic-angle sample spinning (MAS) spectra were obtained with a high-speed MAS probe using 4-mm zirconia rotors that contained approximately 80 mg of sample. Spinning rates of 5 to 12 kHz were used.

Lineshape simulations were performed on a 486 microcomputer using a Fortran-77 program that incorporates the POWDER interpolation routine of Alderman, Solum, and Grant.²¹

Calculations of the phosphorus chemical shielding tensors were performed on a Silicon Graphics Indigo² XL workstation using the Gaussian-92²² and RPAC version 9.0²³ computational packages. The calculations utilized experimental geometries as indicated in the text (except for (CH₃)₃PNH, *vide infra*) and a “locally dense” basis set,²⁴ with 6-311+G(3d) basis sets on P and X (X = B, C, N, O) and a 3-21G basis set for the methyl carbons and all hydrogens, all with standard exponents.

Results and Discussion

Phosphorus-31 Solid-State NMR of Triphenylphosphine–Borane. The ³¹P cross-polarization magic-angle spinning (CPMAS) NMR spectrum of (C₆H₅)₃PBH₃ (**1**) shows a single peak at +21.4 ppm. There is a slight splitting of this peak of

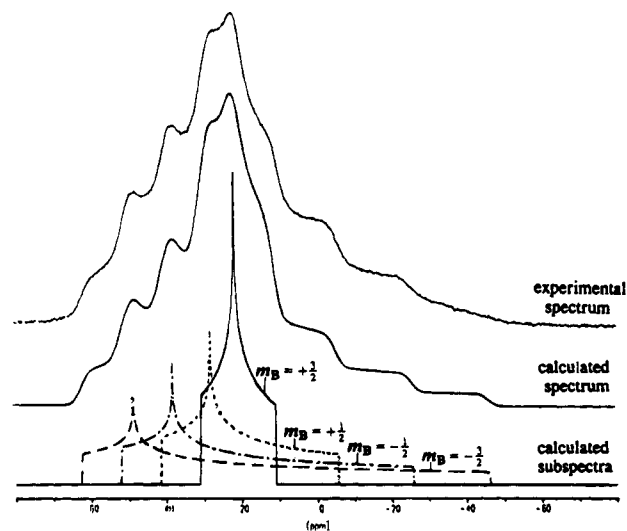


Figure 1. ³¹P CP static NMR spectra of (C₆H₅)₃PBH₃ at 11.7 T: experimental spectrum; calculated spectrum, with 500 Hz line broadening added; and calculated subspectra for each ¹¹B ($I = 3/2$) spin state.

approximately 60 Hz. This is due to J coupling between ³¹P and ¹¹B ($I = 3/2$, 80.42% naturally abundant), in agreement with the reported value of $^1J(^{31}\text{P}, ^{11}\text{B}) = 60$ Hz observed in solution,²⁵ although the outer wings of the expected quartet cannot be resolved. The crystal structure of this compound²⁵ indicates that there are two molecules in the unit cell; however, they are almost superimposable; thus, their ³¹P chemical shielding characteristics are not expected to differ significantly. The ³¹P line width is relatively large, on the order of 100 Hz for each of the two peaks; this may arise from unresolved J -coupling between ³¹P and ¹⁰B ($I = 3$, 19.58% naturally abundant) and line-broadening induced by the quadrupolar interaction of the two nuclear isotopes of the adjacent boron center.

The ³¹P CP powder NMR spectrum of **1** is given in Figure 1, along with the best-fit simulation of the experimental spectrum. The lineshape $\nu_P(\theta, \phi)$ arises from the orientation-dependence (given by the polar and azimuthal angles θ and ϕ with respect to the magnetic field direction) of the ³¹P anisotropic chemical shift and the ³¹P–¹¹B direct dipolar coupling, as well as the relative orientation of these two interactions,²⁶ given by the equation,

$$\nu_P(\theta, \phi) = \nu_0 [1 - (\sigma_{11} \sin^2 \theta \cos^2 \phi + \sigma_{22} \sin^2 \theta \sin^2 \phi + \sigma_{33} \cos^2 \theta)] + m_B R_{PB} [3(\sin \beta \sin \theta \cos(\alpha - \phi) + \cos \beta \cos \theta)^2 - 1] \quad (1)$$

where ν_0 is the ³¹P Larmor frequency, σ_{ii} ($i = 1, 2, 3$) are the principal components of the ³¹P chemical shielding tensor, m_B is the spin state of the adjacent ¹¹B nucleus, R_{PB} is the ³¹P–¹¹B dipolar coupling constant, and the angles α and β are the azimuthal and polar angles, respectively, describing the orientation of the P–B dipolar vector (*i.e.*, the P–B bond) in the principal axis system of the ³¹P chemical shielding tensor. Since ¹¹B has a spin $I = 3/2$, four ³¹P subspectra are observed, corresponding to each of the four possible spin states of the ¹¹B nuclei ($m_B = +3/2, +1/2, -1/2, -3/2$) to which the ³¹P nuclei are dipolar-coupled. In practice, absolute chemical shieldings, referenced to the bare nucleus, are not measured; rather, the chemical shifts relative to an accepted reference compound are determined. Thus, the principal components of the ³¹P chemical

(19) Wasylishen, R. E.; Power, W. P.; Penner, G. H.; Curtis, R. D. *Can. J. Chem.* **1989**, *67*, 1219.

(20) Hansen, Aa. E.; Bouman, T. D. *J. Chem. Phys.* **1985**, *82*, 5035.

(21) Alderman, D. W.; Solum, M. S.; Grant, D. M. *J. Chem. Phys.* **1986**, *84*, 8717.

(22) Frisch, M. J.; Trucks, G. W.; Head-Gordon, M.; Gill, P. M. W.; Wong, M. W.; Foresman, J. B.; Johnson, B. G.; Schlegel, H. B.; Robb, M. A.; Replogle, E. S.; Gomperts, R.; Andres, J. L.; Raghavachari, K.; Binkley, J. S.; Gonzalez, C.; Martin, R. L.; Fox, D. J.; Defrees, D. J.; Baker, J.; Stewart, J. J. P.; Pople, J. A. *Gaussian 92*, Revision A; Gaussian, Inc.: Pittsburgh, PA, 1992.

(23) Bouman, T. D.; Hansen, Aa. E. *RPAC Molecular Properties Package, Version 9.0*; Southern Illinois University at Edwardsville: Edwardsville, IL, 1991.

(24) Chesnut, D. B.; Rusiloski, B. E.; Moore, K. D.; Eglolf, D. A. *J. Comput. Chem.* **1993**, *14*, 1364.

(25) Huffman, J. C.; Skupinski, W. A.; Caulton, K. G. *Cryst. Struct. Commun.* **1982**, *11*, 1435.

(26) Power, W. P.; Wasylishen, R. E. *Annu. Rep. NMR Spectrosc.* **1991**, *23*, 1.

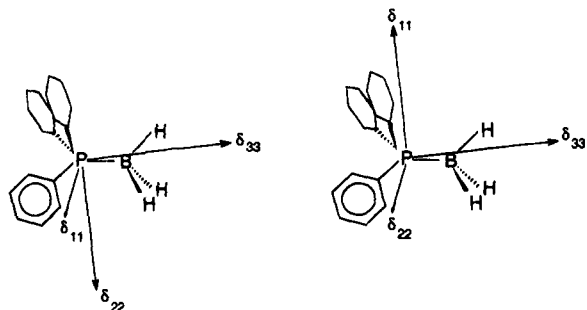


Figure 2. Orientation of the phosphorus chemical shift tensor in $(\text{C}_6\text{H}_5)_3\text{PBH}_3$.

shift tensor, given by δ_{ii} ($i = 1, 2, 3$), are determined experimentally, where δ_{11} corresponds to the least shielded component σ_{11} , *etc.*, in accordance with convention.²⁷ The chemical shift values may be converted to chemical shielding using the absolute chemical shielding scale for phosphorus established by Jameson *et al.*,²⁸ given by

$$\sigma_{ii} = 328.35 \text{ (in ppm)} - \delta_{ii}, \quad (2)$$

where $ii = 11, 22, 33$ or iso.

Simulation of the ^{31}P NMR powder lineshape for **1** provides the three components of the phosphorus chemical shift tensor, $\delta_{11} = 46.6 \pm 0.4$ ppm, $\delta_{22} = 33.2 \pm 0.8$ ppm, and $\delta_{33} = -15.6 \pm 0.4$ ppm. The orientation of the tensor was determined as well, with δ_{33} lying $6.5 \pm 1^\circ$ from the P–B bond and the remaining two components lying approximately perpendicular to this axis. As the dipolar interaction possesses axial symmetry, it is not possible to orient δ_{11} and δ_{22} within an arbitrary rotation about the P–B bond. The nonaxial symmetry of the phosphorus chemical shift tensor is a reflection of the varying twist angles of each of the phenyl rings attached to phosphorus, as determined by the X-ray diffraction study.²⁵ The rings are in a staggered conformation with respect to the BH_3 group. One complete phenyl ring lies essentially in the PBH plane, where the hydrogen is in the *trans* position with respect to the ring. The other two rings are rotated approximately 30° in opposite directions from the equivalent planes with respect to their *trans*-oriented hydrogens. Consequently, the most likely orientation of δ_{11} and δ_{22} is such that one component lies perpendicular to the P–B bond within the nonrotated (phenyl)PBH plane, while the other lies perpendicular to both this plane and the P–B bond. The orientation of the phosphorus chemical shift tensor is depicted in Figure 2.

The ^{31}P – ^{11}B dipolar coupling constant of 2100 ± 50 Hz corresponds to a phosphorus–boron bond length of 1.95 ± 0.02 Å. This is somewhat longer than the reported crystallographic bond length of 1.917 Å determined at -165°C ²⁵ but is still in close agreement. While librational motion might be expected to attenuate the observed dipolar coupling, resulting in a derived bond length that is too long,²⁹ librations are not anticipated to occur to any great extent in this relatively bulky molecule. Another possible contributor to errors in bond lengths that are derived from dipolar coupling constants is anisotropic indirect (or J) spin–spin coupling (ΔJ), which results in an “effective” dipolar coupling, $R_{\text{eff}} = R_{\text{PB}} - \Delta J/3$.³⁰ However, on the basis of the small magnitude of the $^1J(^{31}\text{P}, ^{11}\text{B})$, this is not expected to contribute significantly to the dipolar splittings measured in this study. The P–B bond length determined from the dipolar coupling falls close to the range of values (1.894–1.937 Å)

(27) Mason, J. *Solid State Nucl. Magn. Reson.* **1993**, *2*, 285.

(28) Jameson, C. J.; de Dios, A.; Jameson, A. K. *Chem. Phys. Lett.* **1990**, *167*, 574.

(29) Henry, E. R.; Szabo, A. *J. Chem. Phys.* **1985**, *82*, 4753.

(30) Vanderhart, D. L.; Gutowsky, H. S. *J. Chem. Phys.* **1968**, *49*, 261.

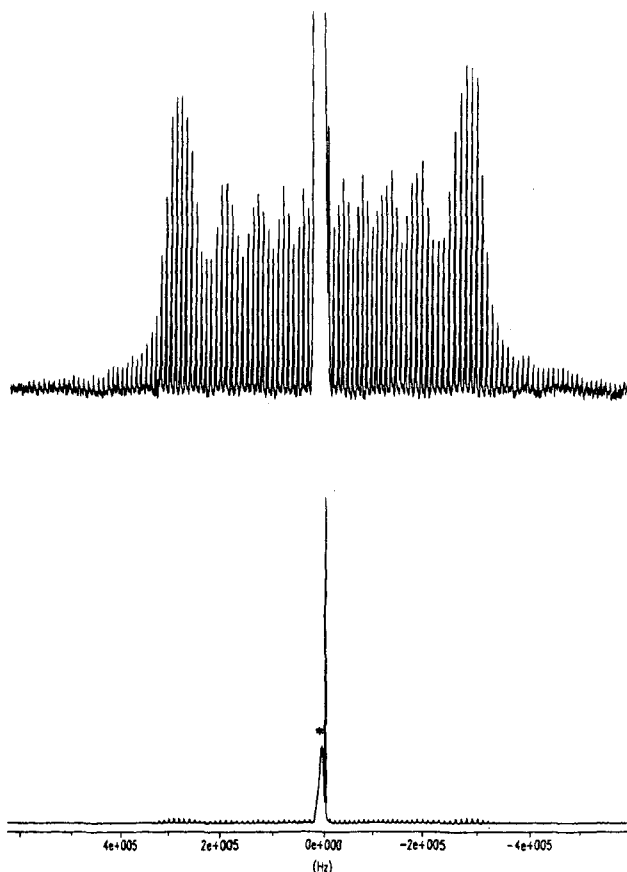


Figure 3. ^{11}B MAS NMR spectrum of $(\text{C}_6\text{H}_5)_3\text{PBH}_3$ at 11.7 T with spinning rate of 10 kHz with a vertical expansion ($\times 16$) of the spectrum given above. The asterisk denotes the background ^{11}B signal due to borosilicate glass in the probe.

determined for other non-halogenated phosphine–borane adducts in the gas phase^{31–33} and in crystalline solids.³⁴

The analysis of the ^{31}P – ^{11}B dipolar coupling assumes that the high-field approximation is valid, *i.e.*, that the ^{11}B Zeeman levels are not perturbed by the quadrupolar interaction. When the quadrupolar interaction becomes comparable in magnitude to the Zeeman interaction, *i.e.*, when the ratio of the Larmor frequency to the quadrupolar coupling falls below 100, the Zeeman energies are no longer eigenstates of the spin Hamiltonian, and the combined Zeeman–quadrupolar Hamiltonian must be used to determine the eigenvalues.³⁵ To verify the high-field approximation, a ^{11}B high-speed MAS NMR spectrum was acquired (see Figure 3) in order to determine the magnitude of the ^{11}B quadrupolar coupling constant. Application of MAS permitted observation of both the satellite and central transitions in spite of the large background signal in the MAS probe due to the borosilicate glass Dewar, the signal of which was not averaged by MAS. The intensity distribution of the spinning sidebands mimics that of the powder lineshape: from the splitting of the most intense features of the satellite region of the spectrum, an estimate of 1.2 ± 0.1 MHz ($\eta_Q = 0$) is derived for the ^{11}B quadrupolar coupling constant. This is in excellent agreement with the ^{11}B quadrupolar coupling constant in trimethylphosphine–borane of 1.198 MHz as determined by Fourier transform microwave spectroscopy.³⁶ At 11.7 T, the

(31) Durig, J. R.; Li, Y. S.; Carreira, L. A.; Odom, J. D. *J. Am. Chem. Soc.* **1973**, *95*, 2491.

(32) Bryan, P. S.; Kuczkowski, R. L. *Inorg. Chem.* **1972**, *11*, 553.

(33) Iijima, K.; Hakamata, Y.; Nishikawa, T.; Shibata, S. *Bull. Chem. Soc. Jpn.* **1988**, *61*, 3033.

(34) McGandy, E. L. Ph.D. Thesis, Boston University, Boston, MA, 1961.

(35) Stoll, M. E.; Vaughan, R. W.; Saillant, R. B.; Cole, T. *J. Chem. Phys.* **1974**, *61*, 2896.

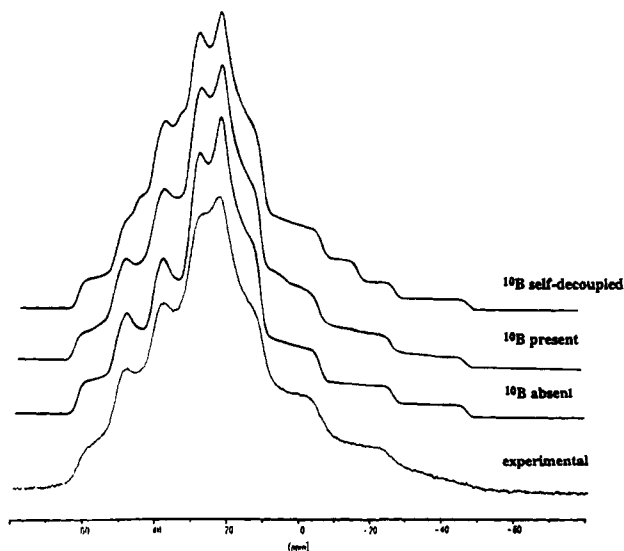


Figure 4. Static powder ^{31}P NMR spectra of $(\text{C}_6\text{H}_5)_3\text{PBH}_3$ at 11.7 T. ^{10}B nuclei are self-decoupled, resulting in an “uncoupled” component of the ^{31}P NMR lineshape. ^{31}P nuclei adjacent to ^{10}B nuclei are dipolar-coupled and observed, ^{31}P nuclei adjacent to ^{10}B nuclei are not observed due to scalar relaxation. Bottom trace is from experimental results.

^{11}B Larmor frequency is 160.62 MHz, resulting in a ratio of this to the quadrupolar coupling that is greater than 130, putting the above analysis of the ^{31}P – ^{11}B dipolar coupling well within the limits of the high-field approximation.

One aspect of the P–B spin-pair that is noticeably absent from the above discussion is the influence of ^{10}B ($I = 3$), which accounts for approximately 20% of naturally occurring boron. It was found that the ^{31}P NMR powder lineshape could be precisely fitted while completely neglecting any interaction with ^{10}B ; however, with the knowledge of the dipolar interaction provided by the ^{31}P – ^{11}B spin-pair, it is possible to determine the origin of the apparent absence of ^{10}B -coupling in the ^{31}P spectrum. Figure 4 provides the calculated spectra corresponding to three distinct possibilities: first, the ^{10}B nuclei are “self-decoupled” from ^{31}P , resulting in a ^{31}P NMR spectrum where 20% of the intensity occurs at frequencies corresponding to the uncoupled or “spin $I = 0$ ” spectrum; second, the ^{10}B is dipolar-coupled to ^{31}P similar to ^{11}B , and scaled according to the ratio of the magnetogyric ratios and the different values of nuclear spin; and finally, the ^{31}P nuclei adjacent to ^{10}B are undergoing scalar relaxation of the second kind in an intermediate regime such that their spectrum is unobservable due to extreme line broadening. It is quite clear that self-decoupling is not occurring, as the “uncoupled” component of the ^{31}P lineshape would be clearly distinguishable in the experimental spectrum, which it is not. It is not possible to distinguish between the latter two possibilities based on the ^{31}P NMR powder lineshape alone. To provide evidence for one of these situations, an intensity calibration experiment was performed, where equimolar amounts of crystalline $(\text{C}_6\text{H}_5)_3\text{P}$ and $(\text{C}_6\text{H}_5)_3\text{PBH}_3$ were ground together, packed in a rotor, and the ^{31}P MAS NMR spectrum was acquired. To ensure the intensities were quantitatively useful, cross-polarization was not used, and the samples were left in the magnet overnight to ensure that $(\text{C}_6\text{H}_5)_3\text{P}$ had reached its ^{31}P Boltzmann equilibrium polarization (the ^{31}P T_1 in $(\text{C}_6\text{H}_5)_3\text{P}$ is approximately 2500 s, that of $(\text{C}_6\text{H}_5)_3\text{PBH}_3$ is approximately 20 s), after which a single pulse was applied, with high-power proton-decoupling during acquisition. The ratio of the intensities was 1:1, providing evidence that the ^{31}P coupled to ^{10}B are present, but their intensity is sufficiently reduced in the ^{31}P NMR powder pattern to preclude identification of their features on the lineshape.

(36) Hillig, K. W.; Kuczkowski, R. L. *Inorg. Chem.* **1987**, *26*, 2232.

Table 1. Isotropic and Anisotropic ^{31}P Chemical Shift Data for Triphenylphosphine and Various Derivatives^a

compound	δ_{11}	δ_{22}	δ_{33}	δ_{iso}	reference
$(\text{C}_6\text{H}_5)_3\text{P}$	9	9	-42	-10	37
$(\text{C}_6\text{H}_5)_3\text{PBH}_3$	47	33	-16	21	this work
$(\text{C}_6\text{H}_5)_3\text{PCHC}(\text{O})\text{H}$	44	12	-6	17	38
$(\text{C}_6\text{H}_5)_3\text{PN}(\text{C}_6\text{H}_5)$	50	31	-85	-1	39
$(\text{C}_6\text{H}_5)_3\text{PO}$	96	96	-104	29	40
$(\text{C}_6\text{H}_5)_3\text{PS}$	107	86	-64	43	41
$(\text{C}_6\text{H}_5)_3\text{PSe}$	98	56	-55	33	41

^a All values are in ppm with respect to 85% $\text{H}_3\text{PO}_4(\text{aq})$ at 0 ppm. They may be converted to chemical shielding values using eq 2.

Table 2. Calculated Principal Components of the Phosphorus Chemical Shielding Tensors for Various Trimethylphosphine Derivatives using the LORG Method with a Locally-Dense 6-311+G(3d)/3-21G Basis Set

compound	σ_{11}	σ_{22}	σ_{33}	σ_{iso}
$(\text{CH}_3)_3\text{P}$	398.2	398.2	426.8	407.7
$(\text{CH}_3)_3\text{PBH}_3$	335.6	335.6	401.8	357.6
$(\text{CH}_3)_3\text{PCH}_2$	324.3	341.4	452.3	372.7
$(\text{CH}_3)_3\text{PNH}$	280.0	315.9	473.5	356.5
$(\text{CH}_3)_3\text{PO}$	278.9	278.9	483.2	347.0

Phosphorus Chemical Shielding in the Isoelectronic Series R_3PX , $X = \text{BH}_3, \text{CH}_2, \text{NH}, \text{O}$. The ^{31}P chemical shift tensor data determined for **1** is presented in Table 1, along with data from the literature for other triphenylphosphine derivatives.^{37–41} For all compounds listed in Table 1, the most shielded component δ_{33} lies approximately along the P–X axis (or direction of the lone pair for $(\text{C}_6\text{H}_5)_3\text{P}$). Of particular interest is the contrast in shielding trends apparent from consideration of isotropic vs anisotropic data. The ^{31}P isotropic chemical shifts range from -10 ppm for $(\text{C}_6\text{H}_5)_3\text{P}$ ³⁷ to 43 ppm for $(\text{C}_6\text{H}_5)_3\text{PS}$,⁴¹ with the isotropic shifts for $(\text{C}_6\text{H}_5)_3\text{PO}$ (29 ppm),⁴⁰ $(\text{C}_6\text{H}_5)_3\text{PBH}_3$ (21 ppm), and $(\text{C}_6\text{H}_5)_3\text{PCHC}(\text{O})\text{H}$ (17 ppm)³⁸ occurring approximately midway between these limits. Strictly on the basis of this information, one might assume that the electronic environments surrounding the phosphorus nuclei in these three compounds were similar. Inspection of the anisotropic parameters shows the dangers in drawing such conclusions from isotropic data alone, as the anisotropic chemical shifts for these compounds are quite different, especially between $(\text{C}_6\text{H}_5)_3\text{PO}$ and $(\text{C}_6\text{H}_5)_3\text{PBH}_3$, which differ by only 8 ppm in their isotropic chemical shifts, yet possess substantially different anisotropies, spanning 200 ppm and 63 ppm, respectively. The much smaller breadth of the ^{31}P chemical shift anisotropy observed for $(\text{C}_6\text{H}_5)_3\text{PBH}_3$ (and $(\text{C}_6\text{H}_5)_3\text{PCHC}(\text{O})\text{H}$) compared to the other compounds in Table 1 is in parallel to the trends in bond lengths between P and the apical atom for these compounds.

The results of *ab initio* calculations of the principal components of the phosphorus chemical shielding tensors for the isoelectronic series $(\text{CH}_3)_3\text{PX}$, where $X = \text{BH}_3, \text{CH}_2, \text{NH}$, and O , as well as the free phosphine $(\text{CH}_3)_3\text{P}$, are presented in Table 2. Previous calculations of phosphorus shieldings have focused on phosphine,^{42–46} other P(III) compounds,^{6,45,47} phosphates,^{6,45,48}

(37) Penner, G. H.; Wasylishen, R. E. *Can. J. Chem.* **1989**, *67*, 1909.

(38) Penner, G. H.; Power, W. P.; Curtis, R. D.; Wasylishen, R. E. *Solid State Nucl. Magn. Reson.* **1992**, *1*, 85.

(39) Power, W. P.; Wasylishen, R. E.; Curtis, R. D. *Can. J. Chem.* **1989**, *67*, 454.

(40) Beml, L.; Clark, H. C.; Davies, J. A.; Fyfe, C. A.; Wasylishen, R. E. *J. Am. Chem. Soc.* **1982**, *104*, 438.

(41) Dutasta, J. P.; Robert, J. B.; Wiesenfeld, L. In *ACS Symp. Ser. 171*; American Chemical Society: Washington, DC, 1981; p 581.

(42) Lazzeretti, P.; Zanasi, R. *J. Chem. Phys.* **1980**, *72*, 6768.

(43) Chesnut, D. B.; Foley, C. K. *J. Chem. Phys.* **1986**, *85*, 2814.

(44) Fleischer, U.; Schindler, M.; Kutzelnigg, W. *J. Chem. Phys.* **1987**, *86*, 6337.

and phosphites,⁴⁹ with no calculations having been reported for phosphine derivatives other than the phosphine oxides.^{6,48} The geometries used for the calculations performed in this study were those reported from experimental gas-phase electron diffraction and/or microwave spectroscopy of $(\text{CH}_3)_3\text{P}$,⁵⁰ $(\text{CH}_3)_3\text{PBH}_3$,³³ $(\text{CH}_3)_3\text{PCH}_2$,⁵¹ and $(\text{CH}_3)_3\text{PO}$.⁵² No experimental geometry has been reported for $(\text{CH}_3)_3\text{PNH}$. Consequently, a direct SCF geometry optimization was performed at the Hartree-Fock level for this compound with a balanced 6-311+G(3d,-2p) basis set for all atoms. The geometry optimization resulted in the following structure: distances (in Å): N-H, 0.996; P-N, 1.545; P-C, 1.815; C-H, 1.082; angles (in degrees): PNH, 117.3; NPC, 114.6; CPC, 103.9; PCH, 110.0; HCH, 108.9; dihedral angles: one hydrogen of each methyl group oriented at 180° with respect to the P-N bond; one methyl oriented at 180° with respect to the N-H bond. The P-N distance and geometry about the phosphorus center agree reasonably well with the experimental geometry reported for (*N*-(trimethylsilyl)imino)trimethylphosphorane.⁵³ The angle at nitrogen in this silyl-substituted compound is not a good model for a simple imine group; comparison with iminotri-*tert*-butylphosphorane⁵⁴ provides a similar PNH angle (114.0°) and N-H distance (1.020 Å). Previous calculations of the phosphorus chemical shielding in phosphine PH_3 ⁴⁶ have shown that the choice of geometry is critical in obtaining reliable calculated values; thus we have opted to use experimental geometries whenever possible.

The calculated phosphorus chemical shielding tensors clearly follow the trends observed experimentally for the triphenylphosphine derivatives discussed previously; the isotropic shifts fall within a relatively narrow range, while the principal components diverge as the substituent X is changed through the isoelectronic series from BH_3 to O. The orientations of the principal components for $(\text{CH}_3)_3\text{P}$, $(\text{CH}_3)_3\text{PBH}_3$, and $(\text{CH}_3)_3\text{PO}$ are determined by the local C_3 symmetry at the phosphorus center, with the most shielded components lying along the P-X bond direction, and the (equivalent by symmetry) least shielded components perpendicular to this axis. The most shielded component, σ_{33} , lies along the P-C bond in the $(\text{CH}_3)_3\text{PCH}_2$ and 2.7° from the P-N bond in $(\text{CH}_3)_3\text{PNH}$. These latter two compounds have no C_3 axis; they possess only mirror or C_2 symmetry. Consequently, the components lying perpendicular to the P-X direction may differ in magnitude. For $(\text{CH}_3)_3\text{PCH}_2$, the least shielded component of the phosphorus chemical shielding tensor lies in the PCH_2 plane perpendicular to the P-C bond, with the intermediate component perpendicular to both this plane and the P-C bond. Conversely, in $(\text{CH}_3)_3\text{PNH}$, the least shielded component is approximately perpendicular to both the PNH plane and the P-N bond, with the intermediate component lying in the PNH plane and approximately perpendicular to the P-N bond. The difference in orientation of the components of least and intermediate shielding for the ylid and

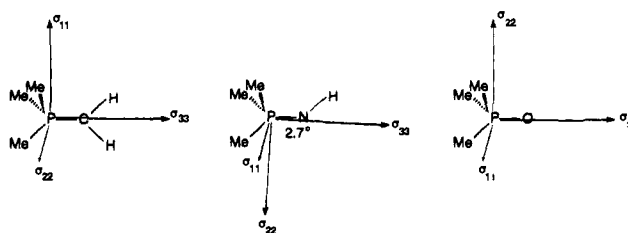


Figure 5. Calculated orientations of the phosphorus chemical shielding tensors for trimethylphosphine oxide, imine, and ylid.

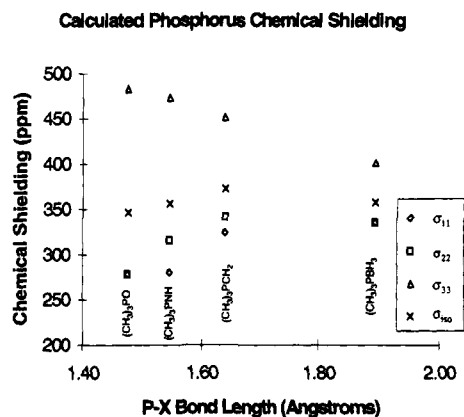


Figure 6. Calculated principal components of the phosphorus chemical shielding tensors of $(\text{CH}_3)_3\text{PX}$, X = BH_3 , CH_2 , NH , O, as a function of the P-X distance.

imine is due to the presence of the nitrogen lone pair in the imine. The magnitude of the least shielded component in the phosphine imine is almost identical to that for the phosphine oxide and is the result of excitations involving lone pair electrons on the adjacent nitrogen or oxygen center in these compounds. In the phosphine ylid, no formal lone pair is present at the carbon center; it more closely resembles the BH_3 group, as evidenced by the similarity in the least shielded components of the phosphorus chemical shielding tensor for these two compounds. The components of the phosphorus shielding tensor lying along the P-X bond become progressively more shielded through the isoelectronic series from BH_3 to O. The orientations predicted in these calculation are depicted in Figure 5.

The calculated principal components have been presented as a function of the P-X bond length for this series of compounds in Figure 6. While no clear relationship exists between the isotropic shift and the P-X distance, distinctly different trends are evident for the principal components parallel and perpendicular to the P-X bond as this bond shortens. The magnitude of the principal components of the phosphorus chemical shielding tensor lying parallel to the P-X bond increases linearly as the bond is shortened, while the magnitude of those components lying perpendicular decreases slightly in shielding. The calculations provide the same explanation as the experimental data concerning the apparent lack of sensitivity of the isotropic chemical shift through this series of compounds; the components of the phosphorus chemical shielding tensor diverge, resulting in averages of their magnitudes which are similar in magnitude and mask the underlying trends.

One consequence of the LORG method for calculation of chemical shielding tensors is the ability to determine individual bond contributions *via* the localized molecular orbitals to the overall chemical shielding observed for a given nucleus. The bond contributions to the total shielding tensor have been summarized in Table 3 in terms of three distinct regions of the phosphorus environment in the $(\text{CH}_3)_3\text{PX}$ series: the phosphorus core (which is further divided into inner and outer regions), the methyl groups, and the lone pair or ligand attached to phos-

(45) Bouman, T. D.; Hansen, A. E. *Chem. Phys. Lett.* **1990**, *175*, 292.

(46) Jameson, C. J.; de Dios, A. C.; Jameson, A. K. *J. Chem. Phys.* **1991**, *95*, 9042.

(47) Gudat, D.; Hoffbauer, W.; Niecke, E.; Schoeller, W. W.; Fleischer, U.; Kutzelnigg, W. *J. Am. Chem. Soc.* **1994**, *116*, 7325.

(48) Tossell, J. A.; Lazzeretti, P. *Chem. Phys. Lett.*, **1987**, *140*, 37.

(49) Farrar, T. C.; Trudeau, J. D. In *Nuclear Magnetic Shieldings and Molecular Structure*; Tossell, J. A., Ed.; NATO ASI Series C: Mathematical and Physical Sciences, Kluwer Academic: Dordrecht, 1993; Vol. 386, p 27.

(50) Bartell, J. S.; Brockway, L. O. *J. Chem. Phys.* **1960**, *32*, 512.

(51) Ebsworth, E. A. V.; Fraser, T. E.; Rankin, D. W. H. *Chem. Ber.* **1977**, *110*, 3494.

(52) Wilkins, C. J.; Hagen, K.; Hedberg, L.; Shen, Q.; Hedberg, K. *J. Am. Chem. Soc.* **1975**, *97*, 6352.

(53) Astrup, E. E.; Bouzga, A. M.; Ostaja Starzewski, K. A. *J. Mol. Struct.* **1979**, *51*, 51.

(54) Rankin, D. W. H.; Robertson, H. E.; Seip, R.; Schmidbaur, H.; Blaschke, G. *J. Chem. Soc., Dalton Trans.* **1985**, 827.

Table 3. Calculated Bond Contributions to the Phosphorus Chemical Shielding in the (CH₃)₃PX Series^a

compound	σ_{11}	σ_{22}	σ_{33}	σ_{iso}
Phosphorus Inner Core Orbitals				
(CH ₃) ₃ P	618.2	618.2	618.4	618.3
(CH ₃) ₃ PBH ₃	619.0	619.0	619.0	619.0
(CH ₃) ₃ PCH ₂	619.0	619.0	619.0	619.0
(CH ₃) ₃ PNH	618.9	618.9	619.0	618.9
(CH ₃) ₃ PO	618.9	618.9	619.0	619.0
Phosphorus Outer Core Orbitals				
(CH ₃) ₃ P	159.9	159.9	117.6	145.8
(CH ₃) ₃ PBH ₃	80.0	80.0	99.8	86.6
(CH ₃) ₃ PCH ₂	60.1	56.7	110.8	75.8
(CH ₃) ₃ PNH	49.1	65.6	115.8	76.8
(CH ₃) ₃ PO	45.5	45.5	117.4	69.5
Methyl Group Orbitals				
(CH ₃) ₃ P	-153.0	-153.0	-327.0	-210.9
(CH ₃) ₃ PBH ₃	-161.0	-164.5	-337.8	-222.3
(CH ₃) ₃ PCH ₂	-167.6	-171.5	-297.7	-212.1
(CH ₃) ₃ PNH	-206.1	-195.6	-327.2	-242.9
(CH ₃) ₃ PO	-224.3	-224.3	-325.8	-257.9
P-X and X Group Orbitals				
(CH ₃) ₃ P	-227.2	-227.2	17.4	-145.6
(CH ₃) ₃ PBH ₃	-199.2	-199.2	20.7	-125.8
(CH ₃) ₃ PCH ₂	-181.8	-159.9	20.6	-106.8
(CH ₃) ₃ PNH	-181.7	-173.2	65.9	-96.3
(CH ₃) ₃ PO	-161.0	-161.0	72.3	-83.1

^a The individual bond contributions have been summed to represent the distinct regions that comprise the phosphorus environment: the inner and outer phosphorus core orbitals, the methyl groups, and the lone pair or ligands (X = BH₃, CH₂, NH, O) attached to phosphorus.

phorus. The total chemical shielding tensor is used rather than the diamagnetic and paramagnetic parts due to the dependence of this division on the choice of gauge origin. As the origin varies for each of the localized molecular orbitals, it is inappropriate to partition the chemical shielding into the two traditional terms proposed by Ramsey⁵⁵ which explicitly assumes a single gauge origin at the nucleus.

Several features concerning the phosphorus chemical shielding become clear upon consideration of the calculated data in Table 3. The inner core orbitals (1s and 2s shells) account for the vast majority of the total chemical shielding, and their contributions are completely isotropic, in accord with their symmetry. The outer core (arising mainly from the 2p shell) also shields the phosphorus nucleus; however, their shielding is anisotropic and changes significantly through the series of derivatives. Note that the sign of the shielding anisotropy for this shell changes from negative to positive between the uncoordinated (CH₃)₃P and the coordinated derivatives and that the anisotropy increases in magnitude through the isoelectronic series. The increase in anisotropy for this shell arises almost exclusively from deshielding of the components perpendicular to the P-X bond direction, with little change in σ_{33} , the component along this axis. The methyl group contributions provide only negative chemical shielding anisotropies, *i.e.*, the component along the P-X bond is always *less* shielded than the components perpendicular to it. Here again, there is little variation in the magnitude of σ_{33} , while both σ_{11} and σ_{22} become progressively less shielded. However, due to the opposite sign of the shielding anisotropy for the methyl groups, this results in a *reduction* of the anisotropy through the isoelectronic series. Finally, the contributions from either the lone pair in (CH₃)₃P or the ligand X in the coordinated phosphines are exclusively shielding, *i.e.*, all components become more shielded through the isoelectronic series, resulting in little change in the anisotropic contributions for the ligands. The differences in the group contributions allow the following conclusions to be drawn:

1. The increase in shielding of the σ_{33} component in the isoelectronic series (CH₃)₃PX arises exclusively from contributions by the ligand X. Contributions from the core orbitals and methyl groups are relatively constant along this component of the chemical shielding tensor.

2. The variations in the magnitudes of σ_{11} and σ_{22} arise from a competition among the contributions of the phosphorus outer core electrons, the methyl groups, and the phosphine ligands. Both the outer core and methyl groups appear to be exclusively deshielding influences on these components, while the ligand is exclusively shielding through the isoelectronic series.

3. The anisotropy of the phosphorus chemical shielding generally increases from BH₃ to O due to the consistent increase in shielding of σ_{33} and the stability (early in the series) or slight deshielding (for NH and O) of σ_{11} and σ_{22} . Thus the chemical shielding anisotropy is predominantly determined by the X group contributions, though not exclusively.

4. Isotropic chemical shifts give a relatively myopic perspective on the changes in shielding that accompany the change in ligands through the isoelectronic series. While one contribution clearly dominates the shielding trends for one component (σ_{33}), the fact that the remaining two components are not dependent on a single contribution results in an isotropic average that does not provide a clear picture of the important influences on the chemical shielding.

Does the increase in the phosphorus chemical shift anisotropies observed experimentally and predicted in the calculations for the isoelectronic series indicate an increase in P-X bond order? For nuclei such as carbon and nitrogen, and even for P(III) species such as the iminophosphines⁴⁷ and diphosphene,⁵⁶ an increase in bond order is accompanied by a significant deshielding of one or two components of the chemical shielding tensor, resulting in an overall deshielding of the isotropic chemical shift. For the P(V) systems investigated here, however, two offsetting effects are observed: the increased shielding of the component lying along the P-X bond, which appears to be directly related to the P-X distance, and the subsequent deshielding of the two components perpendicular to the P-X bond, resulting in little overall change in the isotropic chemical shift. The difference in character between the other multiply bonded systems and the P(V) compounds probably arises from the charge-transfer or dative nature of the interaction between P and X, where the anisotropy of the phosphorus chemical shielding tensor increases with the degree of donation from phosphorus to the attached group. Hence, it appears that a closer association between P and X is reflected by larger chemical shielding anisotropies, but this does not follow the expected trends for increased multiple bonding. A definitive explanation may be provided by a detailed study of the phosphorus chemical shielding surface⁵⁷ and, in particular, the influence of the P-X internuclear separation⁵⁸ for each of these compounds.

"X" Chemical Shielding in the Isoelectronic Series R₃PX, X = BH₃, CH₂, NH, O. Another indication of the degree of P-X bonding may be obtained from the chemical shielding tensors of the attached nuclei, *i.e.*, ^{10/11}B, ¹³C, ^{14/15}N, or ¹⁷O. There is little experimental data concerning the chemical shielding tensors of these nuclei in such compounds. For the stabilized phosphorus ylid, (C₆H₅)₃P¹³CHC(O)OCH₂CH₃, Penner *et al.*³⁸ estimated a carbon chemical shift anisotropy of 100 ± 10 ppm, which they concluded was inconsistent with a description of that carbon as olefinic, since a chemical shift

(56) Zilm, K. W.; Webb, G. G.; Cowley, A. H.; Pakulski, M.; Orendt, A. *J. Am. Chem. Soc.* **1988**, *110*, 2032.

(57) Jameson, C. J. In *Nuclear Magnetic Shieldings and Molecular Structure*; Tossell, J. A., Ed.; Kluwer Academic Publishers: Dordrecht, 1993; p 95.

(58) Jameson, C. J.; de Dios, A. C. *J. Chem. Phys.* **1993**, *98*, 2208.

(55) Ramsey, N. F. *Phys. Rev.* **1953**, *91*, 303.

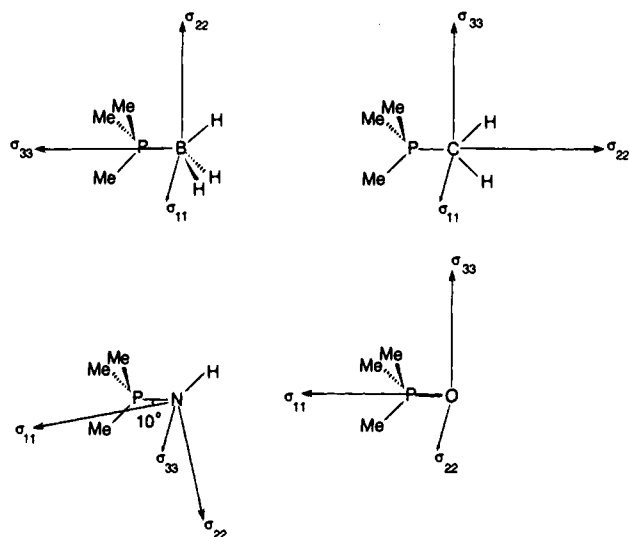


Figure 7. Calculated orientations of the chemical shielding tensors for the boron, carbon, nitrogen, and oxygen nuclei in trimethylphosphine borane, ylid, imine, and oxide, respectively.

Table 4. Calculated Principal Components of the "X" Chemical Shielding Tensors (X = B, C, N, O) for Various Trimethylphosphine Derivatives using the LORG Method with a Locally-Dense 6-311+G(3d)/3-21G Basis Set

compound	σ_{11}	σ_{22}	σ_{33}	σ_{iso}
(CH ₃) ₃ PBH ₃	159.8	159.8	173.3	164.3
(CH ₃) ₃ PCH ₂	205.8	215.3	248.9	223.3
(CH ₃) ₃ PNH	224.4	264.5	266.5	251.8
(CH ₃) ₃ PO	215.8	305.5	305.5	275.6

anisotropy of 200 ppm is typical for an olefinic carbon. In this study of the borane adduct, the anisotropy of the ¹¹B chemical shift tensor was less than 50 ppm estimated from the central transition lineshape of a static powder sample (the background signal of the probe precluded a more quantitative estimate). However, there is no data concerning boron chemical shielding tensors with which to compare this value. The predictions of theoretical calculations of the chemical shielding tensors for boron, carbon, nitrogen, and oxygen for these nuclei in the compounds (CH₃)₃PX are given in Table 4. In none of the cases are large anisotropies typical of multiply-bonded systems predicted by the calculations, indicating that the apparent difference between true multiple-bonding and dative interactions evidenced by the phosphorus chemical shielding is also reflected in the chemical shielding tensors of the adjacent nuclei. As each of the X nuclei possesses some anionic character due to the charge donation from phosphorus, the electronic environment is quite symmetrical, resulting in small chemical shift anisotropies.

The predicted orientations of the principal components for the X chemical shielding tensors are provided in Figure 7. Numerous examples of carbon, nitrogen, and oxygen chemical shielding tensors have been reported.¹³ The orientation and magnitudes of the principal components of the carbon chemical shielding tensor in the phosphine ylid most closely resemble those found for CH₂ groups in alkanes,⁵ bearing no resemblance to those found in alkenes such as ethylene¹⁵ or in carbenes such as the imidazol-2-ylidene.⁵⁹ The orientation of the nitrogen shielding tensor for the phosphine imine is in accord with the findings of divalent nitrogen species, with the intermediate component of the nitrogen shielding tensor approximately along the direction of the nitrogen lone pair and the most shielded

component perpendicular to the plane containing nitrogen and its two adjacent nuclei.⁶⁰ However, the magnitude of the anisotropy at 40 ppm is much smaller than has been observed for amides which are typically 150 ppm. No reports of nitrogen shielding tensors for simple alkylamines have been reported, although the analogy with carbon chemical shielding would lead one to expect that the nitrogen shielding tensor observed for the phosphine imine would be similar to those found in alkylamines. There has been a single report of an ¹⁷O chemical shielding tensor for a carbonyl oxygen in the organic molecule benzophenone,⁶¹ with most existing data pertaining to inorganic oxides or metal carbonyls. In benzophenone, the oxygen shielding tensor is oriented with the least shielded component lying along the C–O bond axis, similar to the situation predicted for trimethylphosphine oxide. The axial symmetry of the phosphine oxide requires the two remaining components to be equivalent and to lie perpendicular to the P–O bond. However, the anisotropy predicted for the phosphine oxide (90 ppm) is significantly smaller than that observed in benzophenone, which spans approximately 1050 ppm. In summary, the chemical shielding characteristics of the "X" nuclei provide no support for the model of multiple bonding in the isoelectronic series R₃PX. Experimental verification of these predictions is currently in progress.

Conclusion

It has been shown that vast differences are exhibited by the principal components of the phosphorus chemical shielding tensors of the series of phosphine derivatives Ph₃PX, X = O, NH, CH₂, BH₃, which are masked in the isotropic data due to the compensating effect of diverging tensor components. As well, the dipolar coupling between ³¹P and the two naturally occurring boron isotopes has been characterized. The coupling to ¹¹B (80.42% natural abundance, *I* = 3/2) provides a measure of the P–B bond length and an axis about which to orient the phosphorus chemical shift tensor. The coupling to ¹⁰B (19.48%, *I* = 3) is unresolvable due to limited intensity but not due to any relaxation effects. The ³¹P chemical shielding tensors of the series of phosphine derivatives R₃PX observed experimentally (for R = C₆H₅) and predicted by *ab initio* calculations (for R = CH₃) appear inconsistent with the model of increasing bond orders through the isoelectronic series X = BH₃, CH₂, NH, and O. In contrast to the expectations based on previous observations of chemical shielding tensors for carbon, nitrogen, and phosphorus(III) multiply-bonded systems, no significant deshielding of the ³¹P chemical shielding occurs. Rather, a tendency to increased shielding along the P–X bond direction prevails as dominant and consistent in these compounds as the P–X bond shortens. The chemical shielding tensors of the adjacent nuclei of the X group also reveal no substantial paramagnetic shielding influences, signaling that the P–X bonding interaction is purely dative in nature, with no multiple-bond character detectable from the nuclear magnetic chemical shieldings.

Acknowledgment. The financial support of NSERC of Canada and the University of Waterloo in the form of operating and equipment grants is gratefully acknowledged. All spectra reported in this work were acquired at the University of Waterloo High-Field NMR Facility, which is also supported by NSERC.

JA943023K

(60) Wasylischen, R. E.; Curtis, R. D.; Eichele, K.; Lumsden, M. D.; Penner, G. H.; Power, W. P.; Wu, G. In *Nuclear Magnetic Shieldings and Molecular Structure*; Tossell, J. A., Ed.; Kluwer Academic Publishers: Dordrecht, 1993; p 297.

(61) Scheubel, W.; Zimmermann, H.; Haebleren, U. *J. Magn. Reson.* **1985**, *63*, 544.

(59) Arduengo, A. J., III; Dixon, D. A.; Kumashiro, K. K.; Lee, C.; Power, W. P.; Zilm, K. W. *J. Am. Chem. Soc.* **1994**, *116*, 6361.